An Error Analysis for the Sampling of Periodic Signals

Mathews Jacob,Thierry Blu and Michael Unser
Biomedical Imaging Group, DMT/IOA
Swiss Federal Institute of Technology Lausanne
CH-1015 Lausanne EPFL, SWITZERLAND
Mathews.Jacob, Thierry.Blu, Michael.Unser@epfl.ch

Abstract— **We analyze the representation of periodic signals in a scaling function basis. This representation is sufficiently general to include the widely used approximation schemes like wavelets, splines and Fourier series representation. We derive a closed form expression for the approximation error in the scaling function representation. The error formula takes the simple form of a Parseval like sum, weighted by an appropriate error kernel. This formula may be useful in choosing the right representation for a class of signals. We also experimentally verify the theory in the particular case of description of closed curves.**

I. Introduction

Classical sampling theory deals with the problem of reconstructing or approximating a signal $s(t)$ from a set of uniform samples or measurements. In its generalized version, the reconstructed approximation [1] is

$$s_h(t) = \sum_{k=-\infty}^{\infty} c_k \varphi\left(\frac{t}{h} - k\right), \qquad (1)$$

where the underlying basis functions are rescaled translates of the generating function φ; h is the sampling step. The generator can be selected so as to yield bandlimited (e.g., $\varphi = \text{sinc}$), spline, or wavelet representations of signals. The expansion coefficients c_k are either determined from the uniform samples of the input signal $s(kh)$, or from a sequence of inner products with a suitable sequence of analysis functions [1]. This theory is well developed for the case in which the input signal is in $L_2(\mathbb{R})$, which also implies that it defined on the whole real line. The approximation quality depends on the sampling step h, the type of algorithm used (e.g., interpolation vs. projection), and most importantly, on the choice of the generating function φ. This can be quantified rather precisely, thanks to the availability of sharp error estimates in the $L_2(\mathbb{R})$ setting [2], [3].

In this paper we are interested in the case where the input signal $s(t)$ is periodic, which is an assumption that is commonly made in practice. When the period T is an integer multiple of the sampling step ($T = Nh$), it is straightforward to adapt most of the L_2 techniques to the periodic case by simply considering periodized basis functions and by redefining the inner product accordingly [4] (see section II). However, the error analysis for signals in $L_2(\mathbb{R})$ is not directly applicable because the square modulus of the Fourier transform is not defined for periodic signals.

Quantitative error analysis of periodic signals will be the main focus of this paper. In particular, we will derive a general predictive error formula that depends on the Fourier coefficients of $s(t)$.

II. Preliminaries

The general formula for determining the expansion coefficients in (1) is

$$c_k = \int_{-\infty}^{\infty} s(\xi)\, \tilde{\varphi}\left(\frac{\xi}{h} - k\right) d\frac{\xi}{h}, \qquad (2)$$

where $\tilde{\varphi}$ is an appropriate analysis function. Here, we assume that $s(t)$ is periodic and that $T = Nh$, where N is a strictly positive integer. Under those conditions, the sequence c_k is periodic as well, with a period N. Furthermore, we can rewrite the synthesis and analysis equations (1) and (2) using N-periodized functions as

$$s_h(t) = \sum_{k=0}^{N-1} c_k \varphi_p\left(\frac{x}{h} - k\right) \qquad (3)$$

$$c_k = \int_0^T s(\xi)\, \tilde{\varphi}_p\left(\frac{\xi}{h} - k\right) d\frac{\xi}{h}. \qquad (4)$$

Combining (3) and (4), we get

$$\begin{aligned} s_h(t) &= \mathcal{Q}_h s(t) \\ &= \sum_{k=0}^{N-1} \left[\int_0^T s(\xi) \tilde{\varphi}_p \left(\frac{\xi}{h} - k \right) d\frac{\xi}{h} \right] \varphi_p \left(\frac{x}{h} - k \right), \end{aligned}$$

where $\mathcal{Q}_h$ is the approximation operator.

III. Computation of the Square Error

The space spanned by the scaling functions are not shift-invariant in general. Hence, the average error at a scale $h = \frac{T}{N}$ is dependent on a time shift on the function $s(t)$. The shifted function is denoted by $s_\tau(t) = s(t - \tau)$.

The mean square approximation error for a shifted function s_τ is given by

$$\gamma_s(\tau, N) = \frac{1}{T} \int_0^T |s_\tau(t) - \mathcal{Q}_N s_\tau(t)|^2 \, dt$$

As the period of the signal is an integer multiple of the sampling step, $\gamma_s(\tau, N)$ is also h-periodic in τ. In most applications, the exact phase of the signal is not known. Hence, we are interested in obtaining a measure of the error that is averaged over τ. This average error is given by

$$\eta_s(N) = \sqrt{\frac{1}{h} \int_0^h \gamma_s(\tau, N) d\tau} \tag{5}$$

The following theorem, which is the main result of this paper, gives an explicit expression for the mean error $\eta_s(N)$.

Theorem 1 *Let $s(t)$ be a T-periodic signal with the Fourier-series coefficients $S(k)$. The mean square approximation error incurred in approximating $s(t)$ as in (5) is given by*

$$\eta_s(N) = \sqrt{\sum_{k=-\infty}^{\infty} |S(k)|^2 E\left(\frac{2\pi k}{N} \right)}, \tag{6}$$

where the approximation kernel $E(\omega)$ depends only on φ and $\tilde{\varphi}$ and assumes the expression

$$\begin{aligned} E(\omega) &= \left| 1 - \hat{\tilde{\varphi}}(\omega)^* \hat{\varphi}(\omega) \right|^2 + \\ & \qquad |\hat{\tilde{\varphi}}(\omega)|^2 \sum_{n \neq 0} |\hat{\varphi}(\omega + 2n\pi)|^2 \qquad (7) \\ &= \underbrace{1 - \frac{|\hat{\varphi}(\omega)|^2}{\hat{a}_\varphi(\omega)}}_{E_{\min}(\omega)} + \underbrace{\hat{a}_\varphi(\omega) \left| \hat{\tilde{\varphi}}(\omega) - \hat{\varphi}_d(\omega) \right|^2}_{E_{\text{res}}(\omega)}, \qquad (8) \end{aligned}$$

where $\hat{a}_\varphi(\omega) = \sum_{k=-\infty}^{\infty} |\hat{\varphi}(\omega + 2n\pi)|^2$ and $\hat{\varphi}_d(\omega) = \frac{\hat{\varphi}(\omega)}{\hat{a}_\varphi(\omega)}$.

Note that this kernel is identical to the one obtained in the case of signals in $L_2(\mathbb{R})$ [2]. When $\tilde{\varphi} = \varphi_d$, the kernel reduces to $E_{\min}(\omega)$ which depends only on φ. The analysis function that gives this minimum error approximation is φ_d (the dual function of φ), as in the case of signals in $L_2(\mathbb{R})$ [5]. This case corresponds to the orthogonal projection.

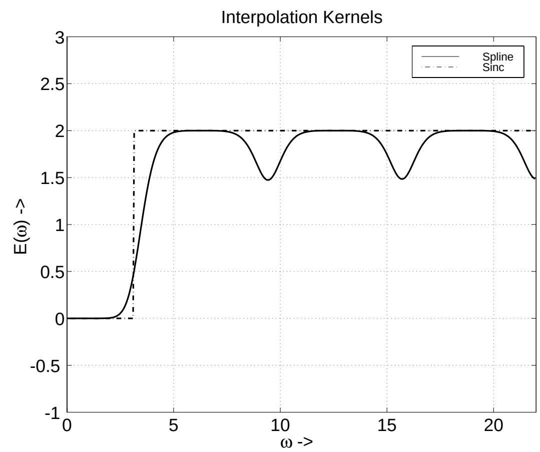

Fig. 1. Error kernels for cubic B-Spline and Sinc representation.

IV. Experimental verification of the error formula

In this section, we validate the expression for the error given by Theorem 1 experimentally. We compare the experimentally measured errors to the theoretical predictions for the approximation of a reference shape as a function of the sampling step h, or equivalently the number of the samples N.

We consider the reference shape as a polygonal representation of the map of Switzerland, with 807 edges. For each experiment, the component functions of the initial piecewise linear model $(x(t), y(t))$ was resampled to a specified number of points.

We considered two types of interpolations of the resampled points: (1) a cubic spline interpolation with $\varphi = \beta^3$ and (2) a bandlimited one with $\varphi = \text{sinc}$. Note that the second approach is equivalent to a truncated Fourier approximation.

The comparisons between the experimental errors and the ones predicted by the theory are given in Fig. 2 and Fig. 3, respectively. It can be seen for both the graphs (Fig. 2 and Fig. 3) that the experimental value of $\sqrt{\gamma_s(\tau, N)}$ for $\tau = 0.5$ is in good agreement with the theoretical prediction $\eta_s(N)$ and oscillate around the theoretical curve.

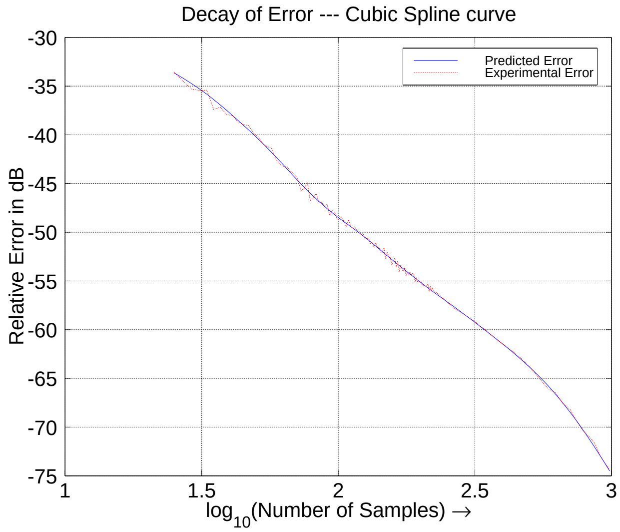

Fig. 2. Decay of the error in interpolation of the map of Switzerland using the cubic spline function

From Fig. 4, it can be seen that the spline interpolation of curves perform slightly better (around 1 dB) than the sinc interpolation. This behavior can be explained with the aid of our error kernel. We can see from Fig. 1 that the spline kernel has lower values as compared to the sinc interpolation kernel when $\omega > \pi$. Hence, at low sampling rates (when the signal has some non-negligible frequency components above π), spline interpolation performs better than the sinc interpolation. The differences tend to vanish as the sampling step decreases.

The map of Switzerland interpolated from 45 samples using the spline and sinc functions are shown in Fig. 5. It can be seen that at some places, the sinc representation results in looping curves. This effect is less likely with the spline representation due to the more local nature of spline interpolation.

V. Conclusion

We have analyzed the representation of periodic signals in a scaling function basis. We obtained an simple and exact expression for the approximation error. This expression may be useful for comparing different scaling functions and to choosing the right one for an application. We have validated the expression in the context of the parametric representation of closed curves; the experimental curves were found to be in excellent agreement with the theoretical prediction.

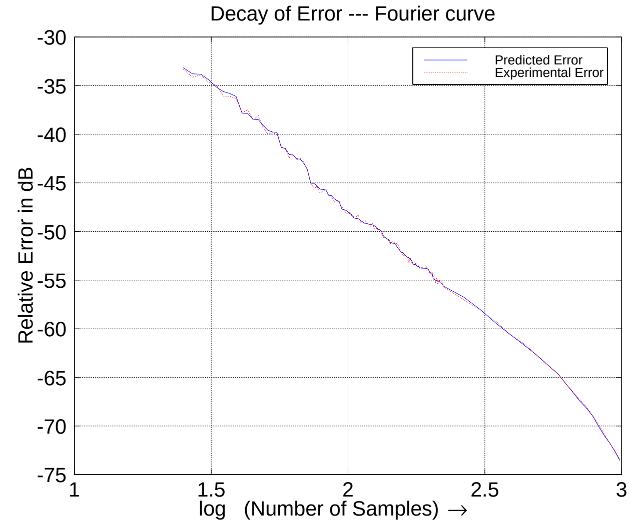

Fig. 3. Decay of the error in interpolation of the map of Switzerland using the Sinc function

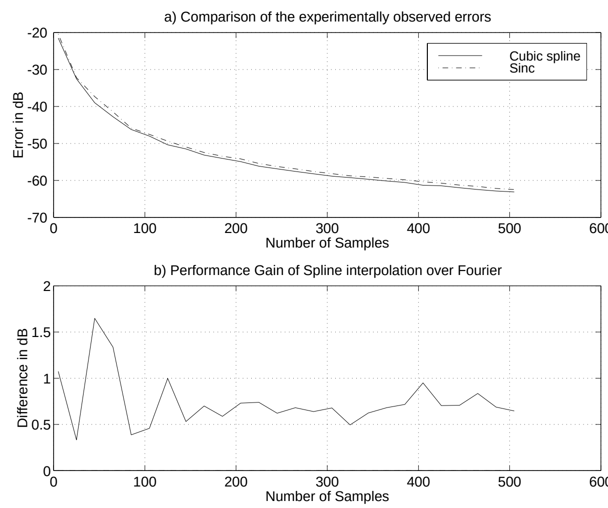

Fig. 4. Comparison of spline and sinc interpolation

Acknowledgements

This work was supported by the Swiss National Science Foundation under grant 2100-053540.

References

[1] M. Unser, "Sampling–50 Years after Shannon," *Proc. IEEE*, vol. 88, pp. 569–587, April 2000.

[2] T. Blu and M. Unser, "Quantitative Fourier analysis of approximation techniques: Part I–Interpolators and projectors," *IEEE Trans. Signal Processing*, vol. 47, pp. 2783–2795, October 1999.

[3] T. Blu and M. Unser, "Quantitative Fourier analysis of approximation techniques: Part II–Wavelets," *IEEE Trans. Signal Processing*, vol. 47, pp. 2796–2806, October 1999.

[4] G.C.H. Chuang and J. Kuo, "Wavelet descriptor of planar curves: Theory and Applications," *IEEE Trans. Image Process.*, vol. 5, pp. 56–70, 1996.

[5] A. Aldroubi and M. Unser, "Sampling procedures in func-

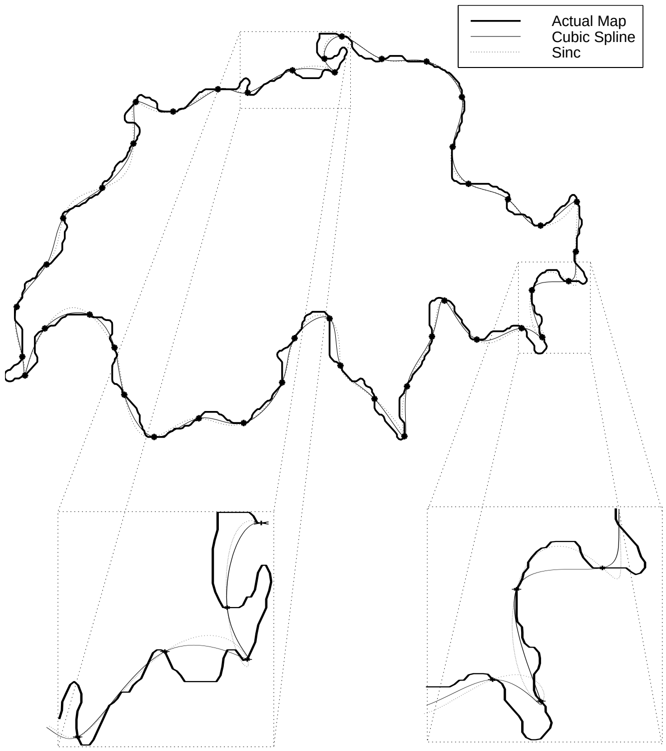

Fig. 5. Actual Map of Switzerland represented using 807 edges is resampled to 45 points (indicated by dots). These points are then interpolated using cubic spline and sinc functions. The graphs below are zoomed portions of the main graph which illustrates the looping nature of sinc interpolation.

tion spaces and asymptotic equivalence with Shannon's sampling theory," *Numer. Funct. Anal. Opt.*, vol. 42, pp. 1–21, March 1994.